Multiband DMRG real time impurity solver

Hans Gerd Evertz, TU Graz


Martin Ganahl

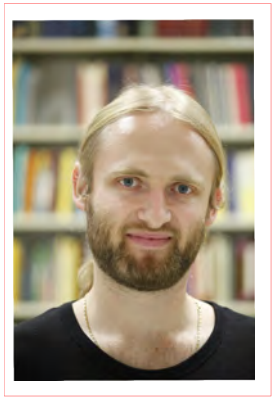
Daniel Bauernfeind


Manuel Zingl


Robert Triebl


Markus Aichhorn

- Hubbard, 2 bands PRB 92, 155132 (2015)
- $SrVO_3$ 3 bands PRX 7, 03101 (2017)
- $SrMnO_3$ 5 bands PRB 97, 115156 (2018)
- Off-diagonal interactions

- Real time: high resolution at all energies
- Can resolve multiplets in Hubbard bands
- As fast as CT-QMC (in cases checked)
- T=0
- no sign problems

Outline

- Introduction and brief summary
- Matrix Product States (MPS): the formalism behind DMRG
  - Efficient representations of a state
  - Time evolution
  - Matrix Product Operators and DMRG
- FTPS: new impurity solver
- Results
  - $SrVO_3$ (3 bands)
  - $SrMnO_3$ (5 bands)
  - Extensions

DMFT: task of an impurity solver

- Band structure from DFT. Construct local Hamiltonian.
- Difficult task in DMFT cycle:

Calculate Green's function for an Anderson impurity model

$$H_{AIM} = H_{loc} + \sum_k V_k \left(c_k^\dagger c_0 + h.c. \right) + \sum_k \epsilon_k n_k$$

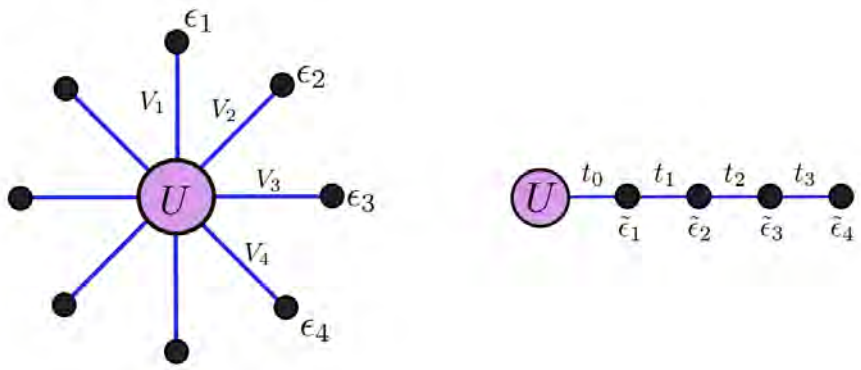

"Star geometry" ↔ Wilson chain

Some current impurity solvers

- **Continuous Time Quantum Monte Carlo (CTQMC):**
  - Precise on imaginary axis
  - Analytic continuation → resolution problems, especially at larger energies
  - Can have sign problem and potentially convergence problems

- **Exact Diagonalization (ED) / Configuration interaction (CI)**
  - Exponential Hilbert space (e.g. N_{bath}= 3 for 3 bands)
  - Low resolution on real frequencies

- **Numerical Renormalization Group (NRG):**
  - Real axis, high resolution at very small energies
  - Low resolution at larger energies

- **Matrix Product States (MPS):**
  - DDMRG: high resolution but slow (separate calculation for every ω)
  - Imaginary time: up to 6 orbitals, but few bath sites and low resolution
  - Real time → good resolution at all energies but multiband appeared expon. difficult

Matrix Product States (MPS)

- Formalism behind DMRG
- **Very efficient representation of states of (mostly) *one-dimensional* systems:**

$$|\psi\rangle = \sum_{\{s_i\}} \underbrace{c_{s_1,\cdots,s_N}}_{=A_1^{s1}\cdot A_2^{s2}\cdots A_N^{sN}} |s_1, s_2, \cdots, s_N\rangle$$

: Ansatz for coefficients: product of matrices

Graphical representation:

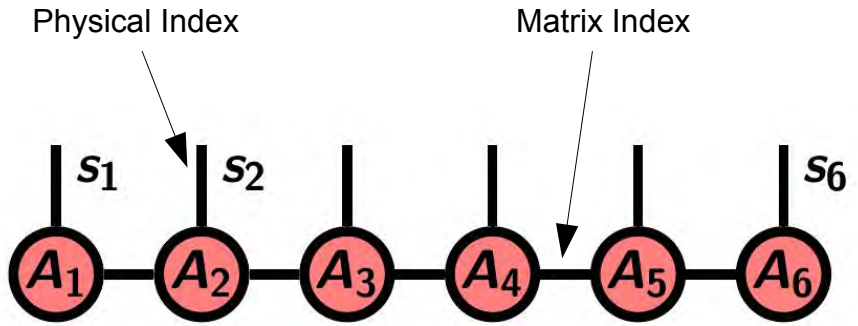

- Ground states by Density Matrix Renormalization Group (DMRG)

  Very precise, e.g. ground state energies exact up to 10 digits for chains of 100 sites
- Real time evolution, nonequilibrium physics, ...

Real time impurity solvers with MPS: strategy

- **To obtain real frequency Green's function:**
  - **Calculate ground state** $|\psi_0\rangle$ of impurity model by DMRG
  - **Time evolve** excitation: $e^{iHt}\ \underline{c\,|\psi_0\rangle}$
  - Calculate overlap: $G^{<}(t) = \underline{\langle\psi_0|\,c^\dagger}\ \ e^{iHt}\ \underline{c\,|\psi_0\rangle}$
  - "Linear prediction", Fourier transform $\rightarrow$ G(ω)

One band:

- Separate the spin-up and spin-down baths: (⇒ lower matrix dimensions)

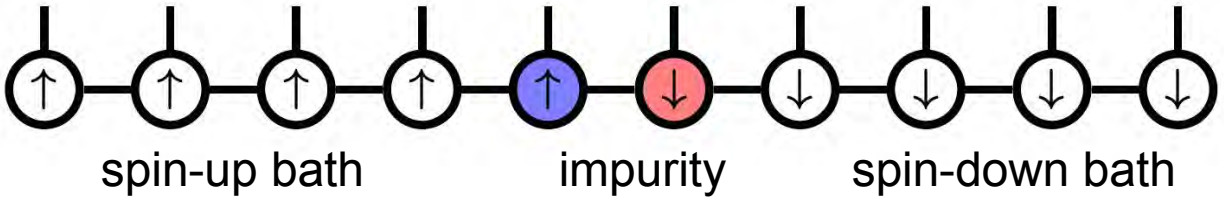

- Large baths (O(100) sites) easily done

Real time impurity Solver with MPS: two bands

- Combine bands into bigger sites
- Works very well for 2 bands

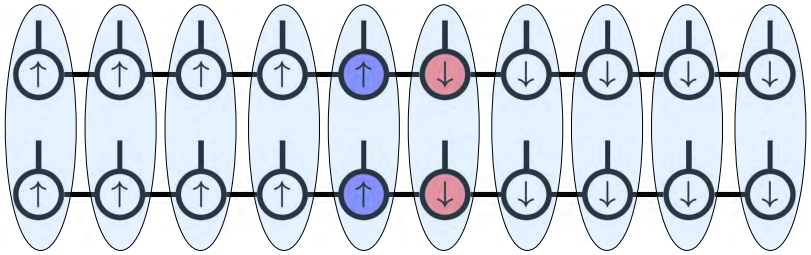

- Examples: DMFT spectrum of Hubbard model on Bethe lattice (Ganahl et al, 2015)

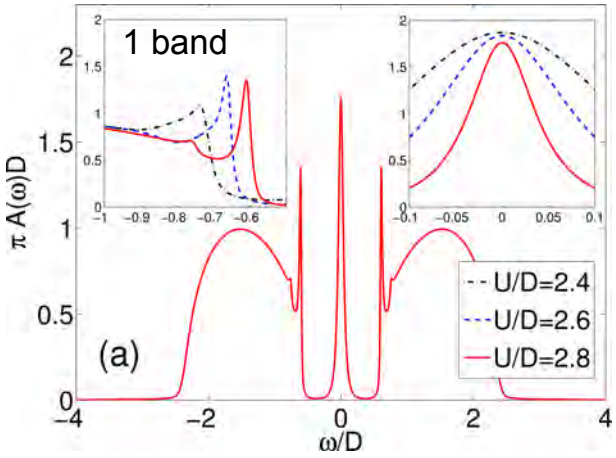

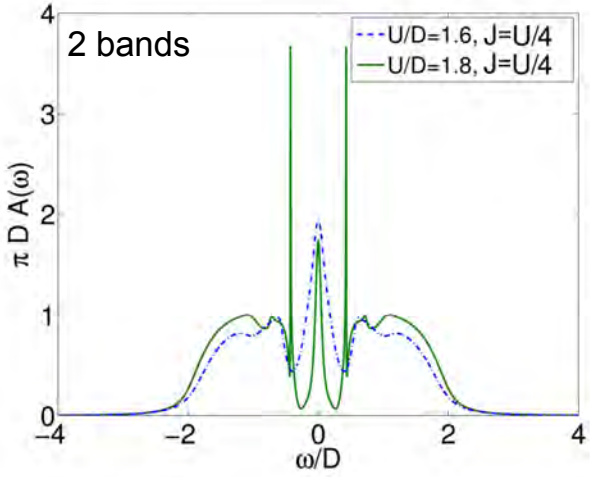

Sharp peaks (invisible in QMC): from interaction of doublon-holon pairs

(Lee, von Delft, Weichselbaum, PRL 2017, one-band model)

- Problem: matrix dimensions m multiply: computational effort ~ $\mathbf{m}^{\mathbf{3 \times n\_bands}}$

  ⇒ **no more than 2 bands feasible this way**

New approach: Fork Tensor Product States (FTPS)

Bauernfeind 2017, 2018

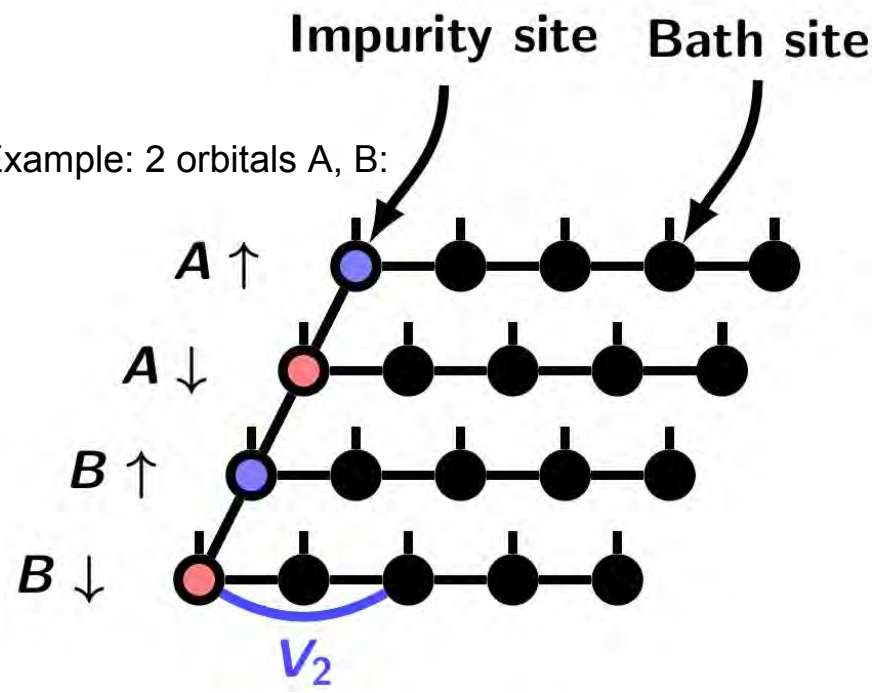

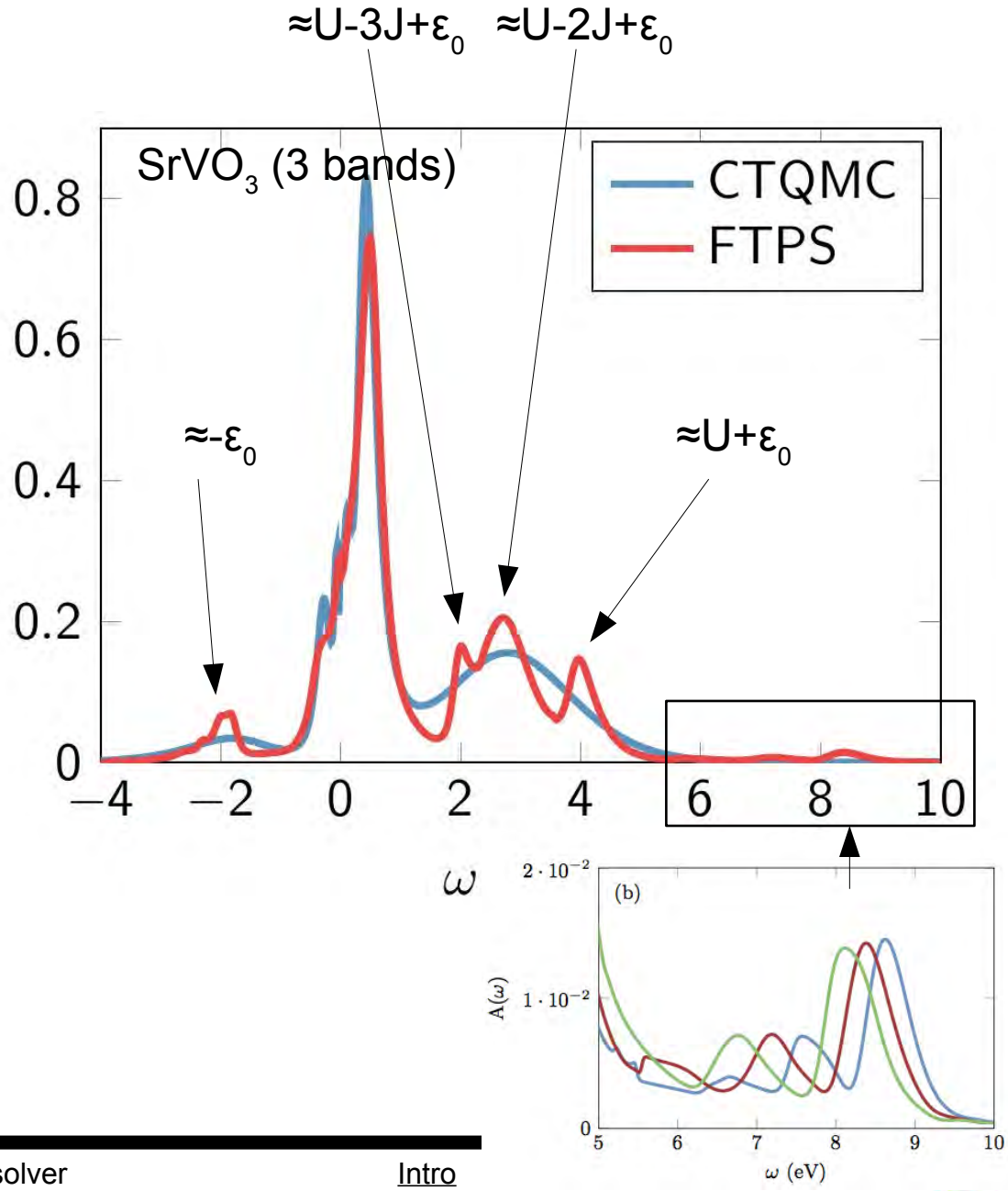

- Real time: high resolution at all energies
- Can resolve multiplets in Hubbard bands
- As fast as CT-QMC (in cases checked)
- T=0
- no sign problems

Matrix Product States

Matrix Product States

Outline:

- **MPS representations of a state**
- **Time evolution**
- **Matrix Product Operators (MPO) and DMRG**

Example: 1d Heisenberg spin chain (equivalent to 1d spinless fermions): 2 states per site

$$\hat{H} = \sum_{i=1}^{L-1} \hat{H}_i \quad \text{with} \quad \hat{H}_i = \frac{J_{xy}}{2}\left[S_i^+ S_{i+1}^- + S_i^- S_{i+1}^+\right] + J_z S_i^z S_{i+1}^z$$

$$\Leftrightarrow \quad \hat{H}_i = t\left(c_j^\dagger c_{j+1} + h.c.\right) + V\,(\hat{n}_j - \frac{1}{2})(\hat{n}_{j+1} - \frac{1}{2})$$

MPS representation of a state

- **Efficient parametrization of 1d states:**

$$|\psi\rangle = \sum_{\{s_i\}} \underbrace{c_{s_1,\cdots,s_N}}_{=A_1^{s1}\cdot A_2^{s2}\cdots A_N^{sN}} |s_1, s_2, \cdots, s_N\rangle$$

: product of matrices

Graphical representation:

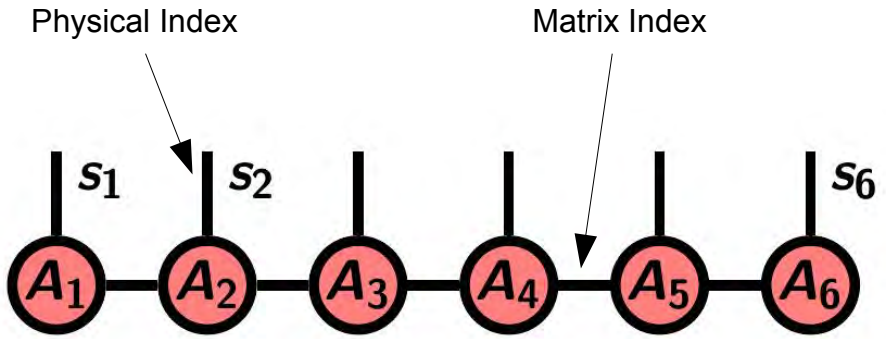

Example : (product state)

$$\begin{array}{rcccccccc} |\psi\rangle & = & | & \downarrow & \downarrow & \uparrow & \downarrow & \uparrow & \downarrow & \rangle \\ j & = & & 1 & 2 & 3 & 4 & 5 & 6 & \\ A_j^{\uparrow} & = & & 0 & 0 & 1 & 0 & 1 & 0 & \\ A_j^{\downarrow} & = & & 1 & 1 & 0 & 1 & 0 & 1 & \end{array}$$

MPS representation of a state

Example: (singlet on 2 sites, entangled state)

$$|\psi\rangle = \frac{1}{\sqrt{2}} \left(|\uparrow\downarrow\rangle - |\downarrow\uparrow\rangle \right)$$

$$A_j^{\uparrow} = (1,0), \quad -\begin{pmatrix} 0 \\ 1 \end{pmatrix}/\sqrt{2}$$

$$A_j^{\downarrow} = (0,1), \quad \begin{pmatrix} 1 \\ 0 \end{pmatrix}/\sqrt{2}$$

Example: (nonlocal singlet)

$$|\psi\rangle = \frac{1}{\sqrt{2}} \left(|\downarrow\downarrow\uparrow\downarrow\downarrow\downarrow\downarrow\downarrow\rangle - |\downarrow\downarrow\downarrow\downarrow\downarrow\downarrow\uparrow\downarrow\downarrow\rangle \right)$$

$$A_j^{\uparrow} = 0, \quad 0, \quad (1,0), \quad \begin{pmatrix} 0 & 0 \\ 0 & 0 \end{pmatrix}, \quad \begin{pmatrix} 0 & 0 \\ 0 & 0 \end{pmatrix}, \quad -\begin{pmatrix} 0 \\ 1 \end{pmatrix}/\sqrt{2}, \quad 0, \quad 0$$

$$A_j^{\downarrow} = 1, \quad 1, \quad (0,1), \quad \begin{pmatrix} 1 & 0 \\ 0 & 1 \end{pmatrix}, \quad \begin{pmatrix} 1 & 0 \\ 0 & 1 \end{pmatrix}, \quad \begin{pmatrix} 1 \\ 0 \end{pmatrix}/\sqrt{2}, \quad 1, \quad 1$$

Main tool: Singular Value Decomposition (SVD)

- *Every m* x *n* matrix *M* can be decomposed as

$$M = U\,D\,V^\dagger$$

with $U^\dagger U = 1$ and $V^\dagger V = 1$

e.g.: M = U D $V^\dagger$

- *D* is diagonal and contains *r* positive *singular values*

$$\lambda_1 \geq \lambda_2 \geq \cdots \geq \lambda_r > \lambda_{r+1} = 0 = \cdots = \lambda_N = 0$$

$$D = \begin{pmatrix} \lambda_1 & & & & & \\ & \ddots & & & & \\ & & \lambda_r & & & \\ & & & 0 & & \\ & & & & \ddots & \\ & & & & & 0 \end{pmatrix}$$

- SVD is very useful to approximate a matrix by neglecting small singular values

(e.g. image compression, signal compression; computational effort $O(\min(mn^2, m^2n))$

- SVD version with *unitary* matrices: $M = \tilde{U}\tilde{D}\tilde{V}^\dagger$

M = U | D — 0 0 0 | $V^\dagger$ / (rest)

Lower rows of $\tilde{V}^\dagger$ do not contribute to *M* because of the zeroes in $\tilde{D}$. They belong to the null space of *M*.

Tool: Schmidt decomposition of a state

- Divide a system arbitrarily into parts A and B
- Generic state $$|\Psi\rangle = \sum_{j,k} c_{jk} |j\rangle_A \; |k\rangle_B$$
- SVD of the coefficients: $$(c_{jk}) = \tilde{U}\tilde{D}\tilde{V}^\dagger$$
- → basis transformation $$|A\rangle_\alpha := \sum_j \tilde{U}_{j\alpha} |j\rangle_A , \quad |B\rangle_\alpha := \sum_k (\tilde{V}^\dagger)_{\alpha k} |k\rangle_B$$
- → Schmidt decomposition

$$|\Psi\rangle = \sum_{\alpha=1}^{\chi} \lambda_\alpha |A\rangle_\alpha \; |B\rangle_\alpha$$

"diagonal" singular values λ_α

$$\text{with } \chi \leq \min(\dim(A), \dim(B)) \quad \text{and} \quad \sum_\alpha \lambda_\alpha^2 = 1.$$

Entanglement between subsystems A and B

- When operator O acts only on A :

$$\langle\psi|\hat{O}|\psi\rangle = \sum_{\alpha\beta} \lambda_\alpha \lambda_\beta \, {}_\alpha\langle B| \, {}_\alpha\langle A|\hat{O}\,|A\rangle_\beta \, |B\rangle_\beta = \sum_\alpha \lambda_\alpha^2 \, {}_\alpha\langle A|\hat{O}\,|A\rangle_\alpha$$

$$= \mathrm{tr}_A \left(\hat{O} \underbrace{\sum_\alpha^\chi \lambda_\alpha^2 |A\rangle_\alpha \, {}_\alpha\langle A|}_{\hat{\rho}_A \ : \ \text{reduced density matrix} \ = \ \mathrm{tr}_B \, \hat{\rho} \ \equiv \ \mathrm{tr}_B \, |\psi\rangle\langle\psi|}\right)$$

- Von Neumann entanglement entropy between A and B :

$$S_A := -\,\mathrm{tr}_A(\hat{\rho}_A \ln \hat{\rho}_A) \ = \ -\sum_\alpha^\chi \lambda_\alpha^2 \ln \lambda_\alpha^2$$

depends only on λ_α

- Maximum possible value: $S_{A,max} = \ln \chi$ (when all λ_α are equal)

→ need matrices up to dimension $\chi \simeq \exp(S_A)$

- Examples: Product state: $|\Psi\rangle = |\uparrow_A \uparrow_B\rangle = |\uparrow\rangle_A \, |\uparrow\rangle_B$: $S_A = 0$: not entangled

Singlet: $|\Psi\rangle = \frac{1}{\sqrt{2}} (|\uparrow\rangle_A \, |\downarrow\rangle_B - |\uparrow\rangle_B \, |\downarrow\rangle_A)$: $S_A = \ln 2$: max. entangled

Exact MPS representation of a state

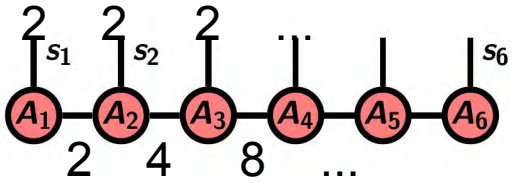

- General state: $|\Psi\rangle = \sum_{s_1 \ldots s_L} c_{s_1 \ldots s_L} |s_1 \ldots s_L\rangle$

- First site: SVD $c_{s_1 (s_2 \ldots s_L)} = \sum_{\alpha_1=1}^{2} \underbrace{\tilde{U}^{[1]}_{s_1 \alpha_1}}_{\text{2x2 matrix}} \lambda^{[1]}_{\alpha_1} \tilde{V}^{\dagger}_{\alpha_1 (s_2 \ldots s_L)}(0)$ with singular values λ_{α_1}

  Also gives Schmidt decomposition between sites 1 and 2

- Second site: SVD $\lambda_{\alpha_1} \tilde{V}^{\dagger}_{\alpha_1 (s_2 \ldots s_L)} = \sum_{\alpha_2=1}^{4} \underbrace{\tilde{U}^{[2]}_{(\alpha_1 s_2) \alpha_2}}_{\text{4x4 matrix}} \lambda^{[2]}_{\alpha_2} \tilde{V}^{\dagger}_{\alpha_2 (s_3 \ldots s_L)}$ with singular values λ_{α_2}

- After site j: $|\Psi\rangle = \sum_{s_1 \ldots s_L} \sum_{\alpha_1}^{2} \sum_{\alpha_2}^{4} \sum_{\alpha_3}^{8} \ldots \; U^{[1]}_{s_1 \alpha_1} U^{[2]}_{(\alpha_1 s_2) \alpha_2} \ldots U^{[j]}_{(\alpha_{j-1} s_j) \alpha_j} \lambda^{[j]}_{\alpha_j} V^{\dagger}_{\alpha_j (s_{j+1} \ldots s_L)} |s_1 \ldots s_L\rangle$

- Rename U → A : $U^{[1]}_{s_1 \alpha_1} U^{[2]}_{(\alpha_1 s_2) \alpha_2} U^{[3]}_{(\alpha_2 s_3) \alpha_3} \cdots =: A^{[1] s_1}_{\alpha_1} A^{[2] s_2}_{\alpha_1 \alpha_2} A^{[3] s_3}_{\alpha_2 \alpha_3} \ldots$

- → Exact MPS: $|\Psi\rangle = \sum_{s_1 \ldots s_L} \sum_{\{\alpha_i\}} A^{[1] s_1}_{\alpha_1} A^{[2] s_2}_{\alpha_1 \alpha_2} A^{[3] s_3}_{\alpha_2 \alpha_3} \ldots A^{[L-1] s_{L-1}}_{\alpha_{L-2} \alpha_{L-1}} A^{[L] s_L}_{\alpha_{L-1}} |s_1 \ldots s_L\rangle$

- But: maximum dimension $2^{L/2}$ (!?!) in the middle (by doing SVD from left and from right)
  Really: matrix dimensions O(100) are enough ! (see later)

Canonical representation and normalization

- Write singular values explicitely, by defining matrices Γ :

$$A^{[j]s_j}_{\alpha_{j-1}\,\alpha_j} =: \lambda^{[j-1]}_{\alpha_{j-1}}\,\Gamma^{[j]s_j}_{\alpha_{j-1}\,\alpha_j} \quad \text{and also} \quad B^{[j]s_j}_{\alpha_{j-1}\,\alpha_j} := \Gamma^{[j]s_j}_{\alpha_{j-1}\,\alpha_j}\,\lambda^{[j]}_{\alpha_j}$$

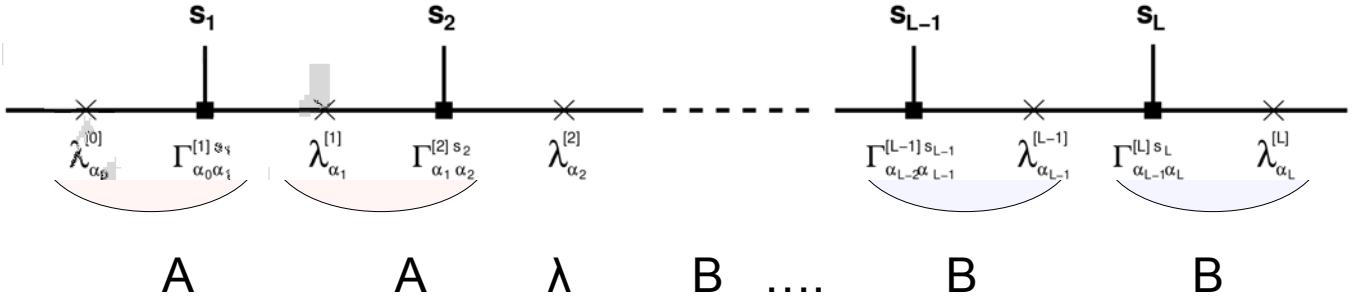

Provides Schmidt decomp. and reduced density matrix at any lattice bond

- Normalization: write $U^\dagger U = 1$ and $V^\dagger V = 1$ graphically:

Expectation value of a local operator

$$\langle\Psi|\hat{O}^{[j]}|\Psi\rangle = \sum_{\{s\},\{s'\}} \langle s'_1 \dots s'_L| \dots \lambda^{*[j]}\Gamma^{*[j]s'_j}\lambda^{*[j-1]} \dots \; O^{[j]}_{s_j s'_j} \; \dots \lambda^{[j-1]}\Gamma^{[j]s_j}\lambda^{[j]} \dots |s_1 \dots s_L\rangle$$

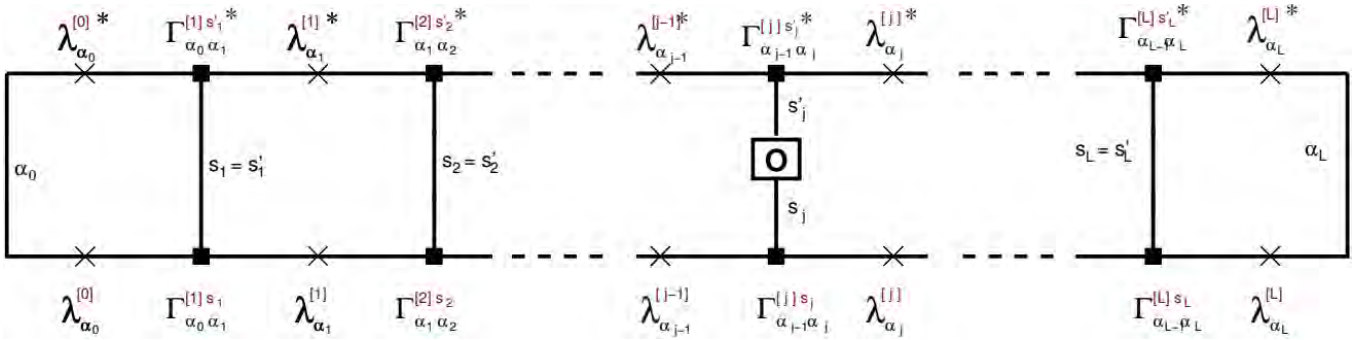

Simplifies because of normalizations and becomes a ***local*** object

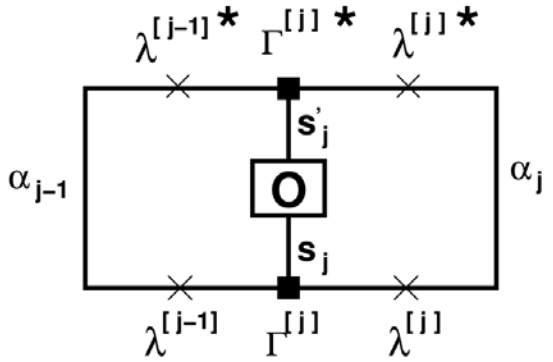

For 1d chains, **small** matrices are enough !

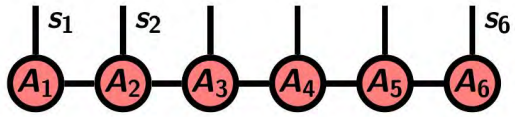

- In 1D, entanglement between “left” and “right” subsystem goes through a single bond

  → entanglement entropy S is small, up to only ln(system size N) (*for ground states*)

  → need only matrix dimensions $\chi = O(N) = O(100)$

- But excited states (time evolution) may need much more

- In higher dimensions: $\mathrm{S}_{max} \sim L^{D-1}$ → exponentially large matrices

- In practice, **truncate matrices** by discarding small singular values,

  either to a maximum size (uncontrolled error),

  or by limiting the “truncated weight” $t_w := \sum_\alpha \lambda_\alpha^2$ of the discarded directions to e.g. 10^{-10}

Time evolution

- H with nearest neighbor coupling: split $\hat{H} = \hat{H}_{even} + \hat{H}_{odd} = \sum_{j,odd} \hat{H}_j + \sum_{j,even} \hat{H}_j$

  such that $e^{-i\hat{H}_{even}t} = \prod_{j,even} e^{-i\hat{H}_j t}$ and $e^{-i\hat{H}_{odd}t} = \prod_{j,odd} e^{-i\hat{H}_j t}$

  2-site operators

- Trotter-Suzuki: $e^{-i\hat{H}t} = \left(e^{-i\hat{H}_{even}\Delta t}\, e^{-i\hat{H}_{odd}\Delta t}\, e^{-i\hat{H}_{even}\Delta t} \ldots e^{-i\hat{H}_{even}\Delta t}\right)(1 + \mathcal{O}(\Delta t))$

  (other operator sequences are possible)

- 2-site operators can be applied locally

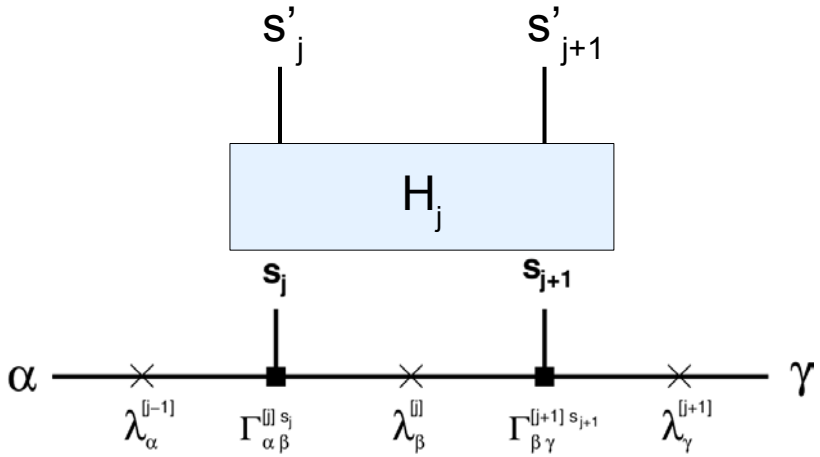

- Matrix dimensions would double at each step → truncate back

Some real time evolutions (an aside)

- Bound state propagation
  of a ↑↑ spin pair
  in Heisenberg groundstate
  (J_z =1.2) (Ganahl PRL 2012)
  → dedicated cold atom
  experiment

FM: S_z

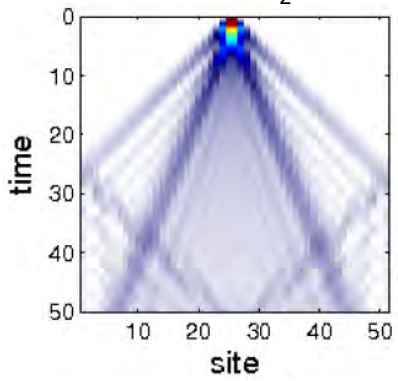

FM: entanglement

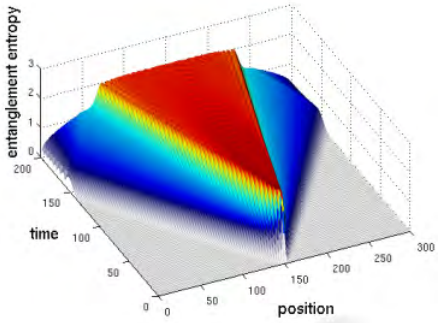

AF: S_z

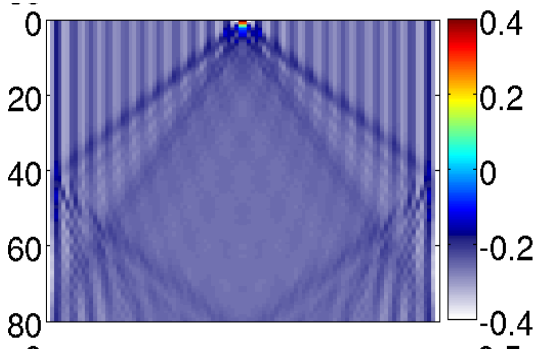

- Scattering between a moving particle
  and a bound state of 10 particles,
  which is shifted left by **2** sites (Ganahl 2013)
  Later reproduced in Bethe ansatz
  (Vlijm, Ganahl 2015)

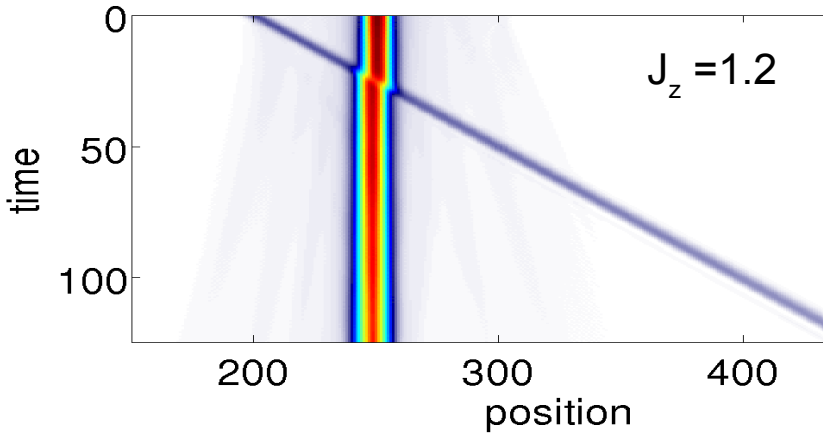

2 bound particles:

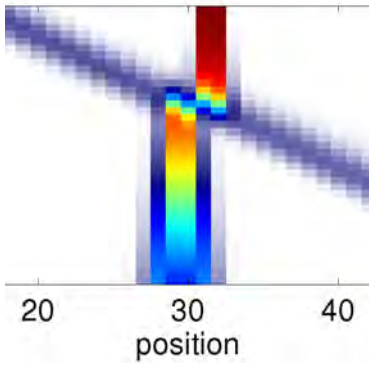

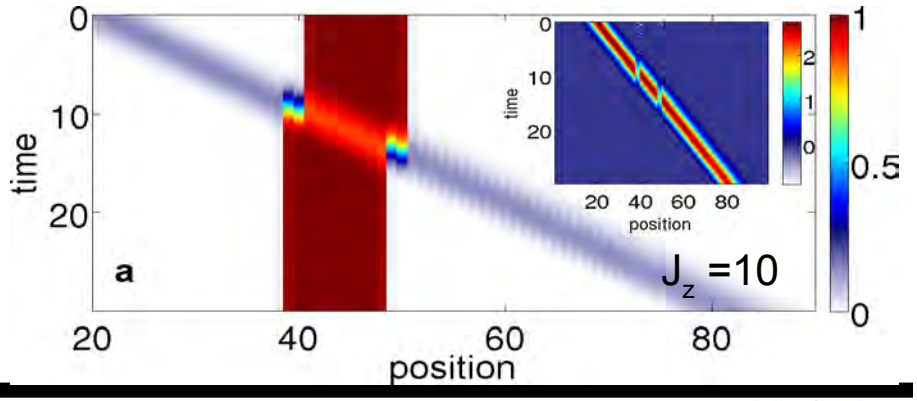

Matrix Product Operators (MPO) and DMRG

- Same approach as for states

$$\hat{O} = \sum_{\{s_i\},\{s_i'\}} W^{s_1,s_1'} W^{s_2,s_2'} \dots W^{s_L,s_L'} \, |s_1', s_2', \dots, s_L'\rangle \langle s_1, s_2, \dots, s_L|$$

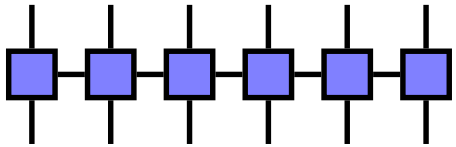

- DMRG: find ground state. Sequentially optimize each MPS matrix A, by finding minimum λ of $H_i^{eff} \; A^{[i]} = \lambda \; A^{[i]}$,

Graphically:

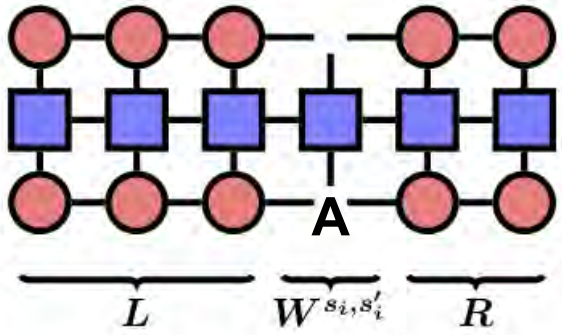

Example: MPO for Anderson Impurity Model

$$H = \sum_{k\sigma} \epsilon_k n_{k\sigma} + \sum_{k\sigma} V_k \left(c^\dagger_{0\sigma} c_{k\sigma} + h.c. \right) + \sum_{\sigma} \epsilon_0 n_{0\sigma} + H_{int}$$

- Choose geometry and numbering

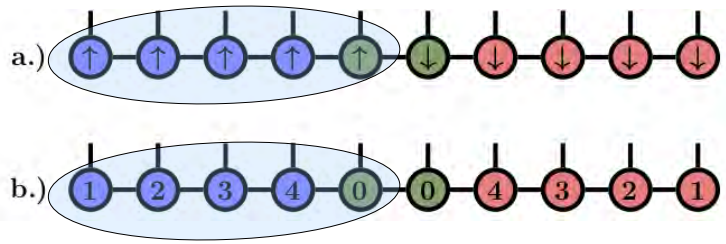

- Solution for MPOs (without H_{int})

$$W_{1\uparrow} = \begin{pmatrix} \epsilon_1 n_{1\uparrow} & 1 & V_1 c_{1\uparrow} & V_1 c^\dagger_{1\uparrow} \end{pmatrix}$$

$$W_{k>1,\uparrow} = \begin{pmatrix} 1 & 0 & 0 & 0 \\ \epsilon_k n_{k\uparrow} & 1 & V_k c_{k\uparrow} & V_k c^\dagger_{k\uparrow} \\ 0 & 0 & p & 0 \\ 0 & 0 & 0 & p \end{pmatrix}$$

with $p = (-1)^n$ for fermion anticommutation

Impurity Solvers

Real time **impurity solvers** with MPS: strategy

(reminder)

- **To obtain real frequency Green's function:**
  - **Ground state** $|\psi_0\rangle$ of impurity model by DMRG
  - **Time evolve** excitation: $e^{iHt}\ c\,|\psi_0\rangle$
  - Overlap: $G^{<}(t) = \langle\psi_0|\, c^{\dagger}\ e^{iHt}\ c\,|\psi_0\rangle$
  - "Linear prediction", Fourier transform → $G(\omega)$

Real time → small times easiest
→ high energies easiest

One band:

- Separate the spin-up and spin-down baths: (⇒ lower matrix dimensions)

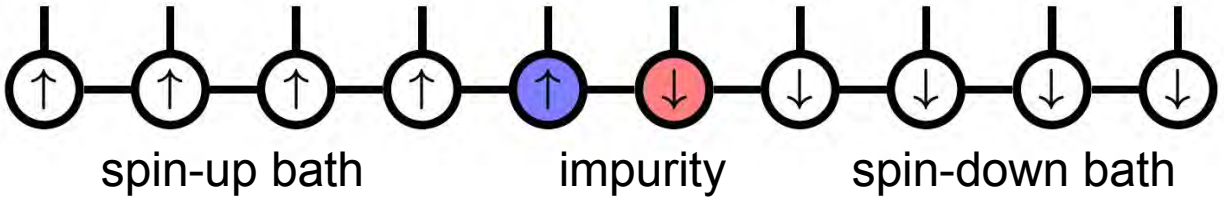

- Large baths (O(100) sites) easily done

Real time impurity Solver with MPS: two bands

(reminder)

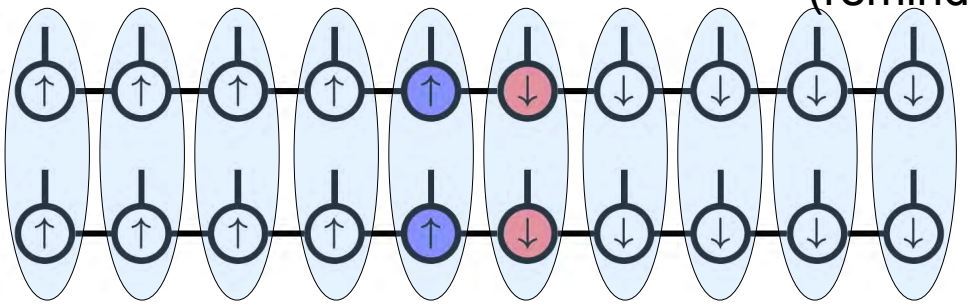

- Combine orbitals into bigger sites
- Works very well for 2 bands

- Examples: DMFT spectrum of Hubbard model on Bethe lattice (Ganahl et al, 2015)

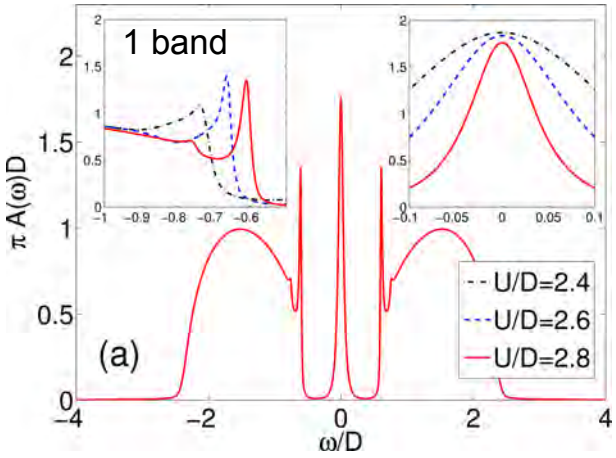

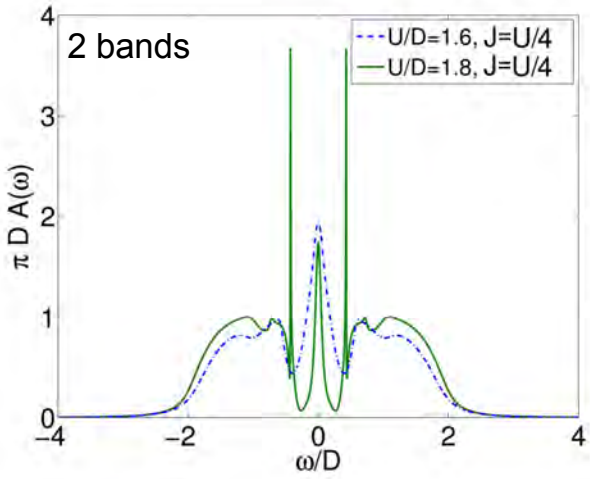

Side-peaks: (invisible in QMC): from interaction of doublon-holon pairs

(Lee, von Delft, Weichselbaum, PRL 2017, one-band model)

- Problem: matrix dimensions m multiply: computational effort ~ $m^{3 \times n\_orbital}$

  ⇒ **no more than 2 bands feasible this way**

New approach: Fork Tensor Product States (FTPS)

Bauernfeind 2017, 2018

Example: 2 orbitals A, B:

- Separate the bands of the bath
  → small bath matrices
- Tree tensor network, bipartition at any bond
  ⟶ DMRG, Time Evolution etc. possible
- Tradeoff: Entanglement at impurity
- "Star geometry" (no Wilson chains):
  ⟶ lower entanglement, much faster

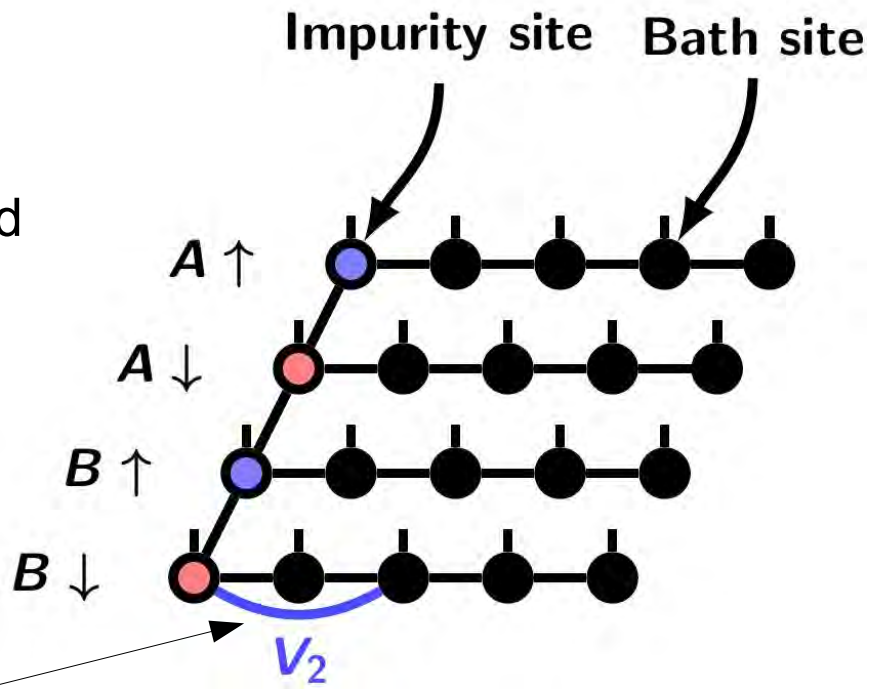

$$V_k \left(c_k^\dagger c_0 + h.c. \right) + \epsilon_k n_k$$

Tree tensor: see also Holzner et al, PRB 2010 (2 orbital NRG)

Kanamori Hamiltonian

$$H = H_{\rm loc} + H_{\rm bath} \tag{1}$$

$$H_{\rm loc} = \epsilon_0 \sum_{m\sigma} n_{m0\sigma} + H_{\rm DD} + H_{\rm SF} + H_{\rm PH}$$

$$H_{\rm DD} = U \sum_{m} n_{m0\uparrow} n_{m0\downarrow} + (U-2J) \sum_{m'>m,\sigma} n_{m0\sigma} n_{m'0\bar{\sigma}} + (U-3J) \sum_{m'>m,\sigma} n_{m0\sigma} n_{m'0\sigma}$$

$$H_{\rm SF} = J \sum_{m'>m} \left(c^\dagger_{m0\uparrow} c_{m0\downarrow} c_{m'0\uparrow} c^\dagger_{m'0\downarrow} + \text{h.c.} \right)$$

$$H_{\rm PH} = -J \sum_{m'>m} \left(c^\dagger_{m0\uparrow} c^\dagger_{m0\downarrow} c_{m'0\uparrow} c_{m'0\downarrow} + \text{h.c.} \right)$$

$$H_{\rm bath} = \sum_{ml\sigma} \epsilon_l n_{ml\sigma} + V_l \left(c^\dagger_{m0\sigma} c_{ml\sigma} + \text{h.c.} \right),$$

$$H_{\rm free} := H_{\rm bath} + \epsilon_0 \sum_{m\sigma} n_{m0\sigma} \tag{2}$$

Bath parameters ϵ_l , V_l from **arbitrary discretization ($\longleftrightarrow$ energy resolution)** of $\Delta(\omega)$

FTPS: adapt methods

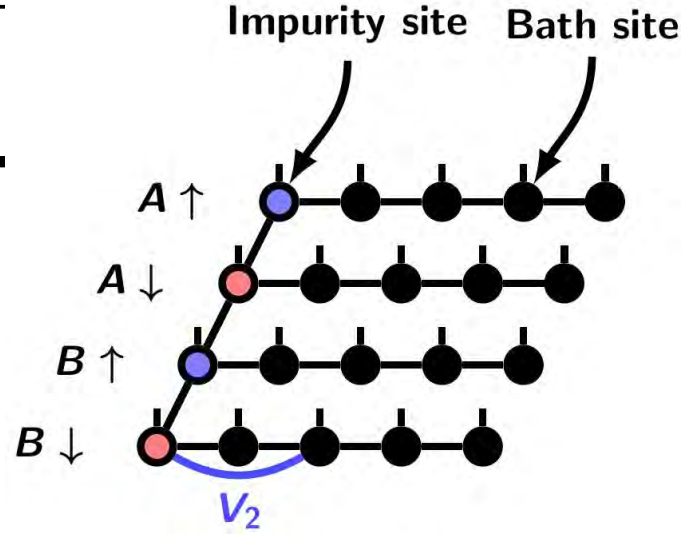

- SVDs: combine tensor indices to get matrices → computational effort up to $O(m_I^3\, m_B)$,

  where m_I: matrix dim. between impurities, m_B : matrix dim. to last bath site)

- Ground state: construct MPOs (FTPOs) for H and use DMRG

  Expensive: $O(m_I^3\, m_B^3)$

Time evolution:

$$e^{-i\Delta t H} \approx \left(\prod_{m'>m} e^{-i\frac{\Delta t}{2}\left(H_{\mathrm{SF}\,m,m'}+H_{\mathrm{PH}\,m,m'}\right)}\right) e^{-i\frac{\Delta t}{2}H_{\mathrm{DD}}} e^{-i\Delta t H_{\mathrm{free}}} e^{-i\frac{\Delta t}{2}H_{\mathrm{DD}}} \left(\prod_{m'>m} e^{-i\frac{\Delta t}{2}\left(H_{\mathrm{SF}\,m,m'}+H_{\mathrm{PH}\,m,m'}\right)}\right)$$

Construct and apply FTPOs for each time evolution operator (→ size up to 6 x 10)

Time evolution of bath

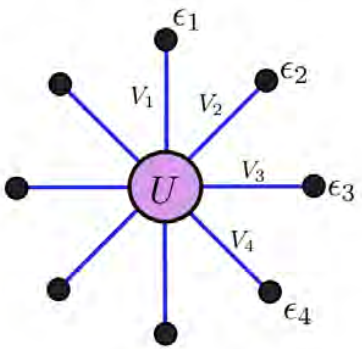

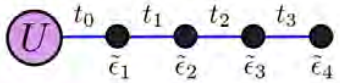

"Star geometry" ↔ Wilson chain

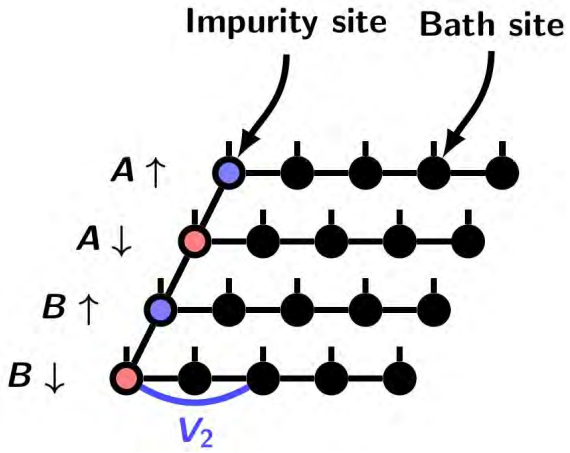

- Use star geometry
- Map onto chain → non-local hoppings (!)
- Treat by "moving impurity through bath and back"
- Achieve much smaller Trotter errors than in Wilson chain:

  → Bath evolution faster by factor 100 for same precision

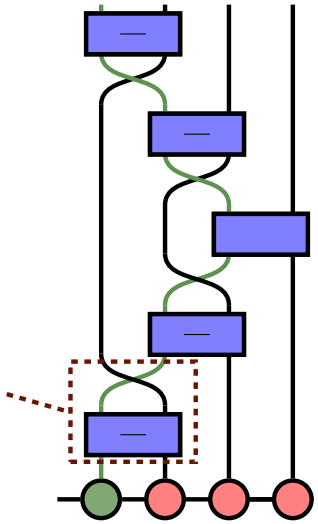

Results

Results: $SrVO_3$

Phys. Rev. X 7, 031013 (2017)

- 3 band model (t_{2g} subspace), Kanamori-Hamiltonian
- Large bath (109 bath sites for each orbital-spin combination, converged)
- Time evolution up to $16eV^{-1}$, T=0
- First: results with only density-density interactions:

- Very good agreement with CTQMC
  (also on imaginary time axis)
- FTPS only:
  3-peak structure in upper Hubbard band

Not resolved by MaxEnt

CPU time for one DMFT iteration:
FTPS: 80h, CTQMC: 32h

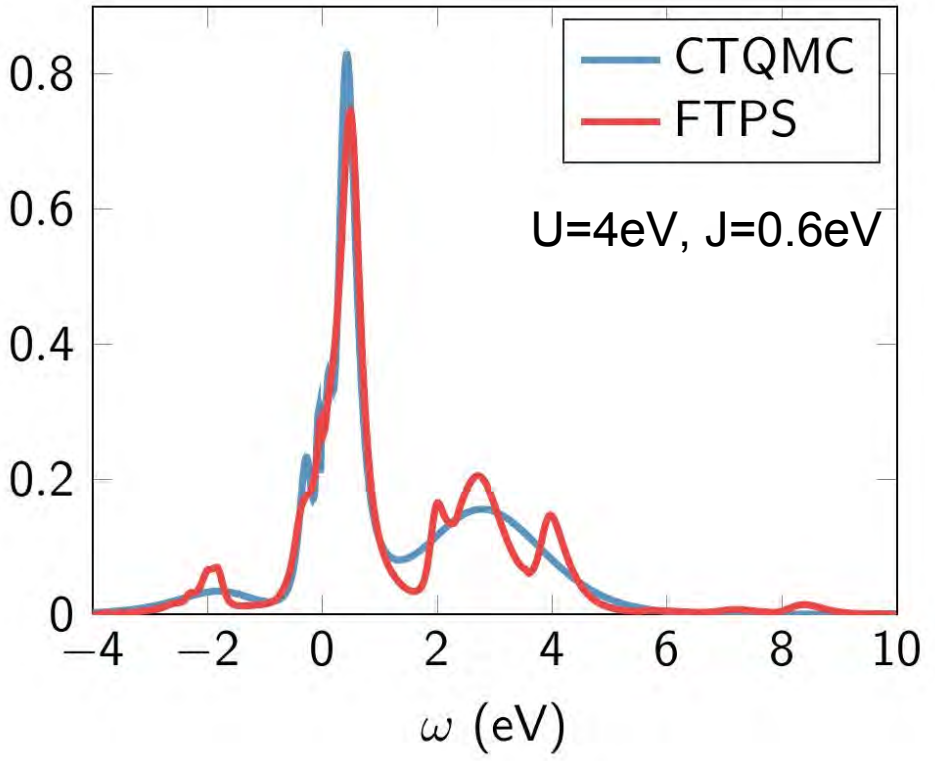

$SrVO_3$: multiplet in upper Hubbard band

- FTPS can resolve multiplets
- Related to atomic energies

particle sector	atomic eigen energies	state
0	ε_0	$\|0,0,0\rangle$
1	0	$\|\uparrow,0,0\rangle$
2	U - 3J+ε_0	$\|\uparrow,\uparrow,0\rangle$
	U - 2J+ε_0	$\|\uparrow,\downarrow,0\rangle$
	U +ε_0	$\|\uparrow\downarrow,0,0\rangle$
3	3U - 9J + 2ε_0	$\|\uparrow,\uparrow,\uparrow\rangle$
	3U - 7J + 2ε_0	$\|\uparrow,\uparrow,\downarrow\rangle$
	3U - 5J + 2ε_0	$\|\uparrow\downarrow,\uparrow,0\rangle$

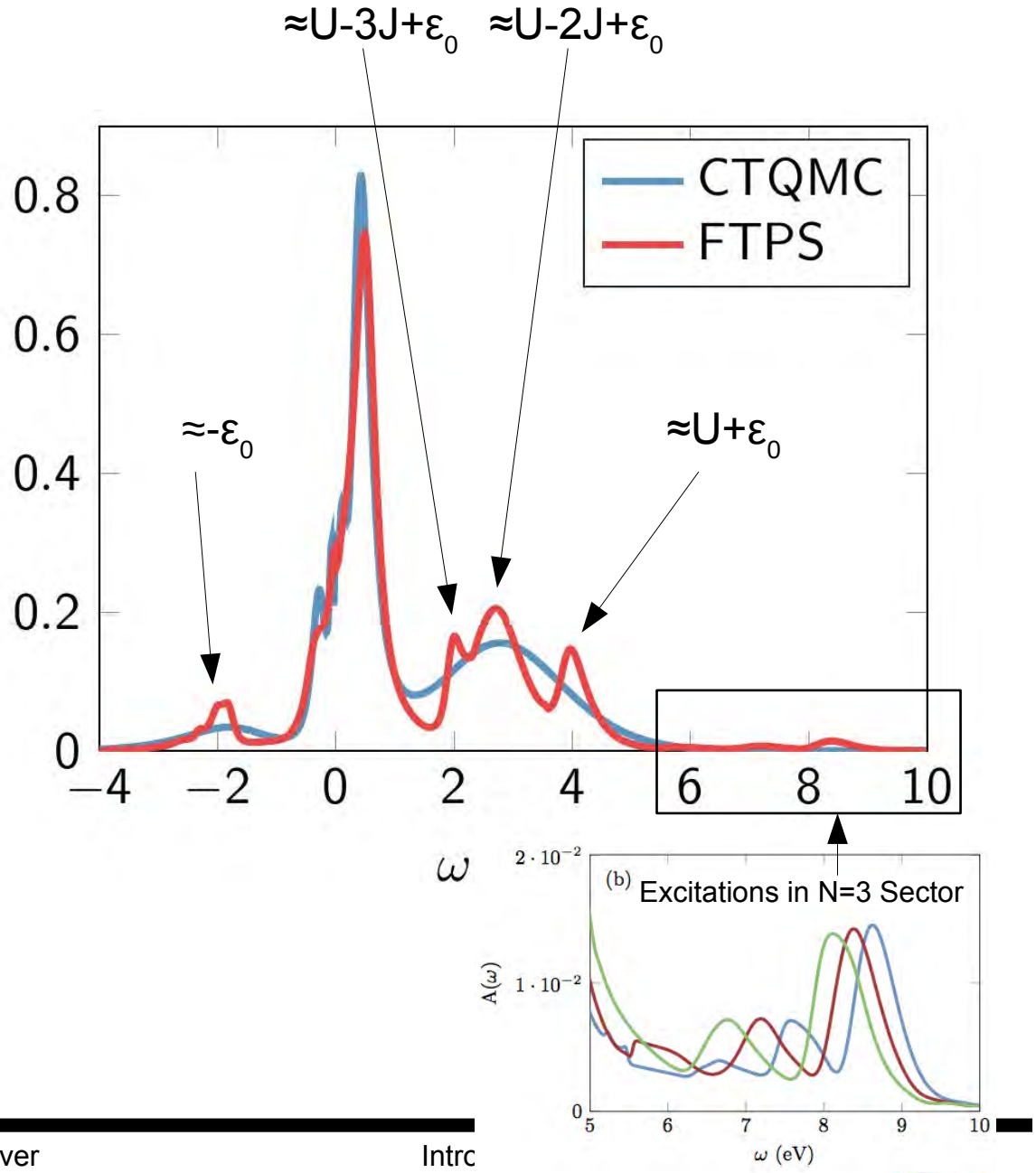

$SrVO_3$: upper Hubbard band for different J

- Interactions ⇒ broadened and shifted peaks

- Can be described by effective $J_{eff} \neq J$

  J= 0.5 eV → J_{eff} = 0.59(6) eV
  J= 0.6 eV → J_{eff} = 0.66(3) eV
  J= 0.7 eV → J_{eff} = 0.72(2) eV

- Central peak almost constant

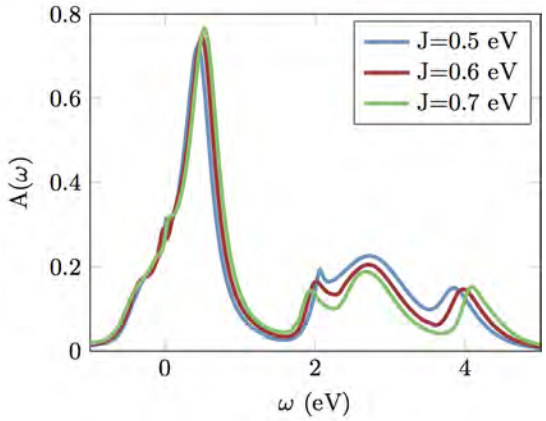

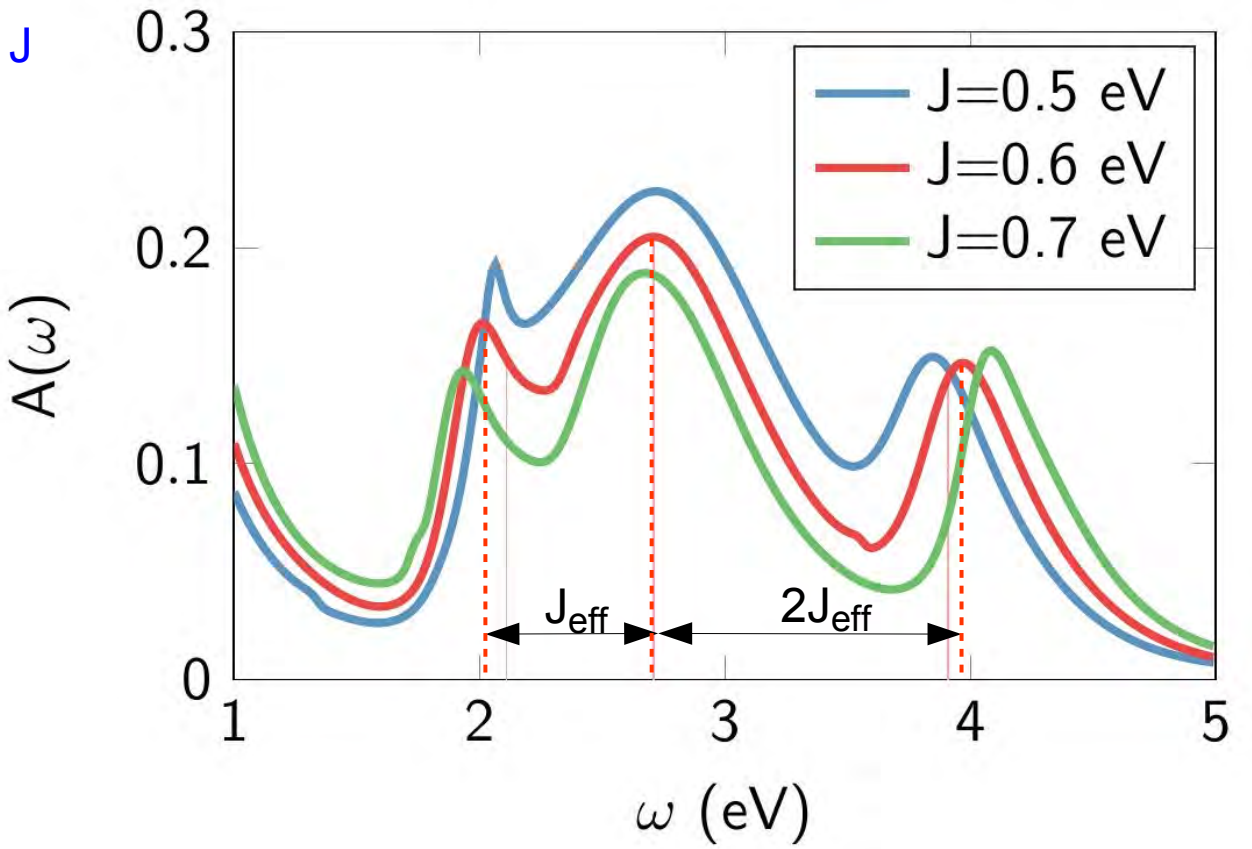

$SrVO_3$: full rotational symmetry

Include spin flip and pair hoppings

Only affect N=2 sector →
Hole excitation and quasi particle peak do not change

Different multiplets due to different atomic eigenstates/eigenenergies.

Energy differences 2J and 3J

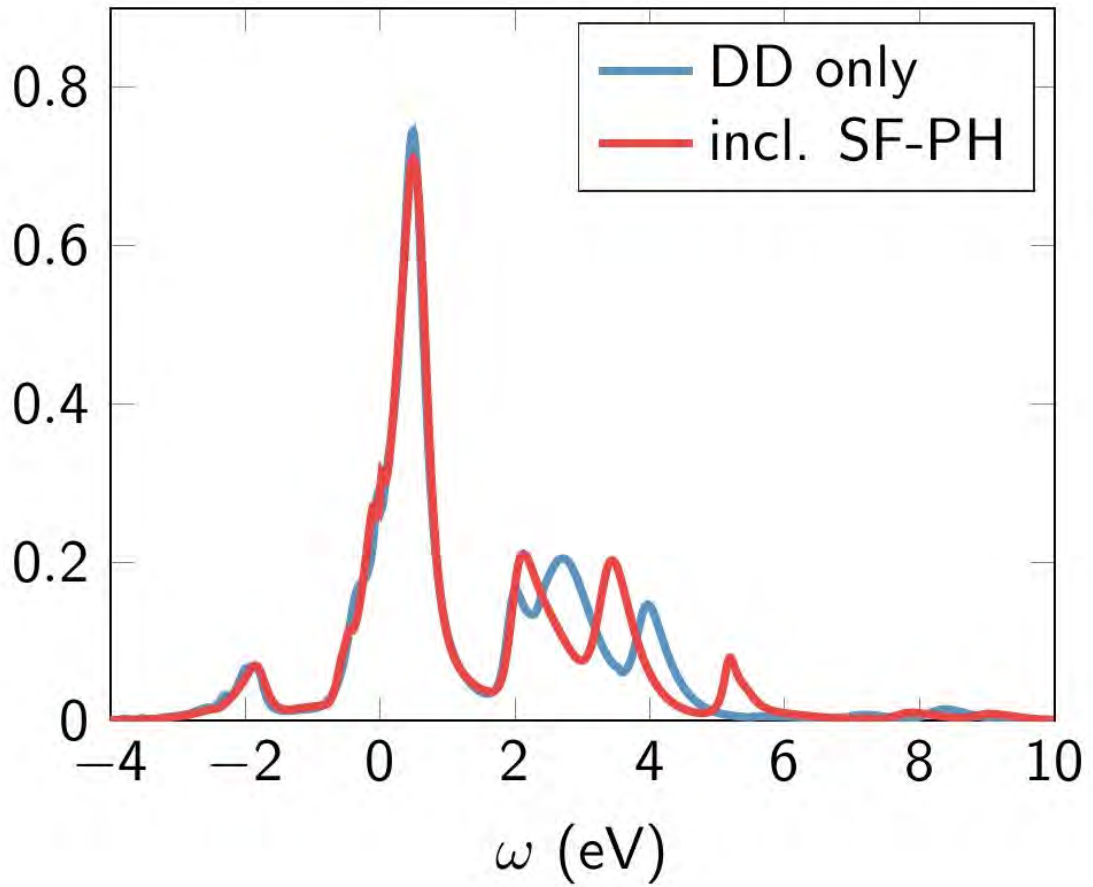

$SrMnO_3$

- 3 electrons in Mn-3d orbitals. Mott Insulator with $|GS\rangle \approx |\uparrow,\uparrow,\uparrow\rangle + |\downarrow,\downarrow,\downarrow\rangle$

- DFT-DOS:

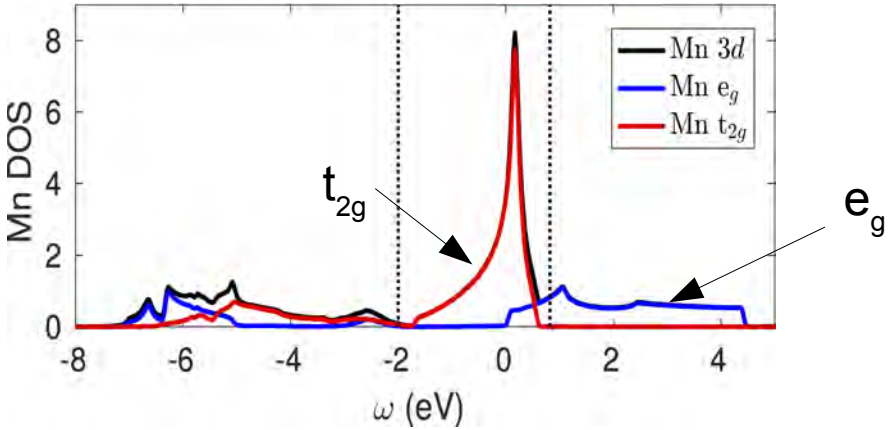

- **e_g orbitals largely above E_F → "unoccupied"**
  Is e_g important ?

- Strong hybridizations with oxygen p-states in lower Hubbard band

  → Use wide energy window [-10eV, 5eV]
  for Wannier projection
  GS then mixes N=3 and N=4 sectors

DMFT: **t_{2g} only**

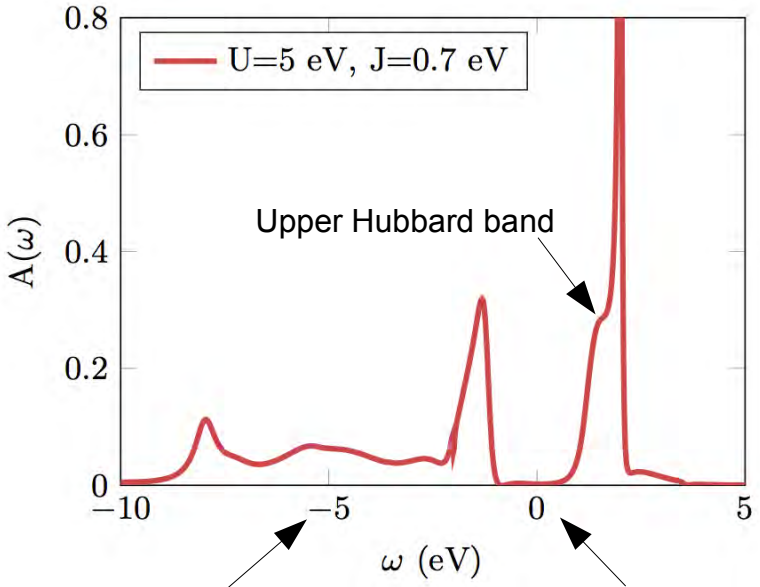

$SrMnO_3$: t_{2g} and e_g orbitals

- Full 5-band calculation (U=6.0, J=0.8)

DMFT: t_{2g} plus e_g

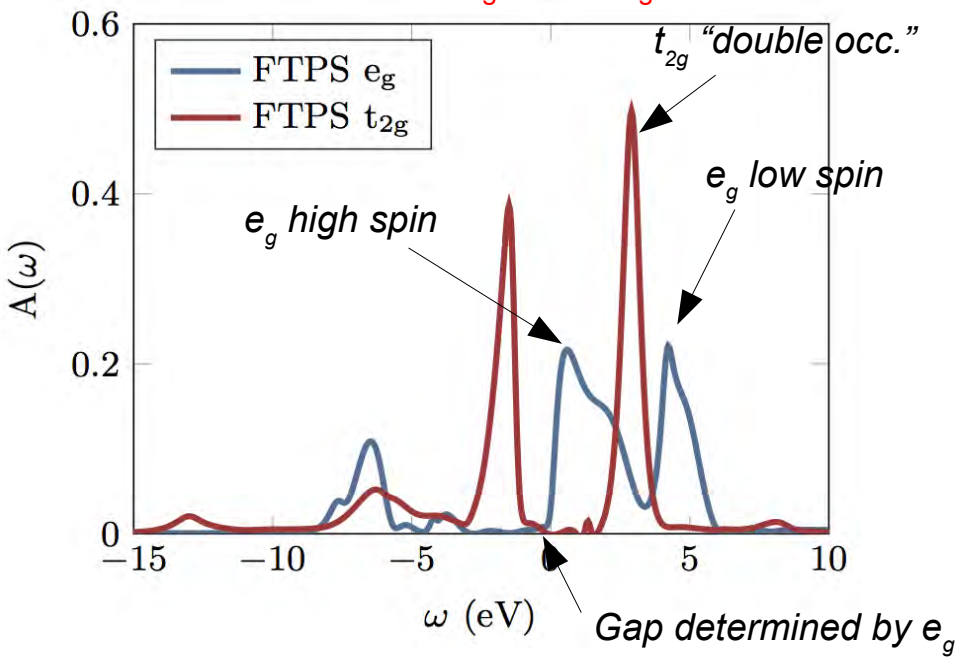

t_{2g} only

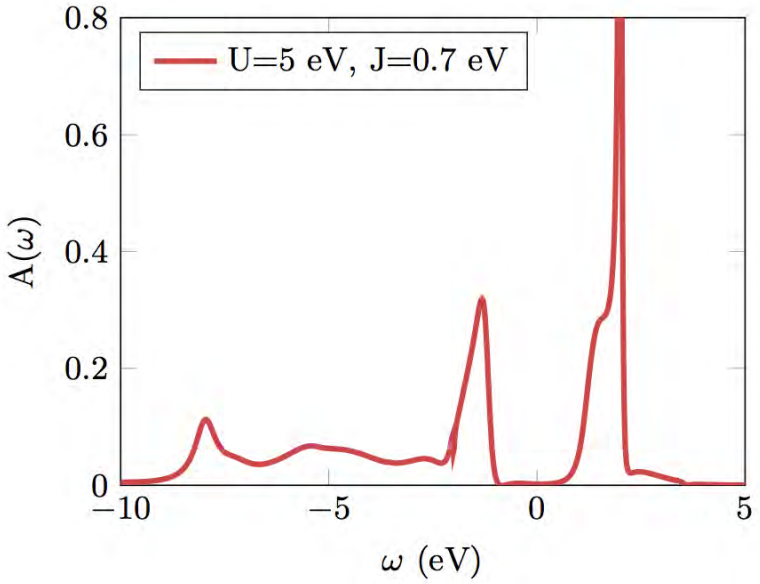

$SrMnO_3$: t_{2g} and e_g orbitals

- Full 5-band calculation (U=6.0, J=0.8)

- e_g is important:
  - determines the gap
  - creates 3-peak structure above E_F
    (not resolved by CTQMC)

Comparison to CTQMC

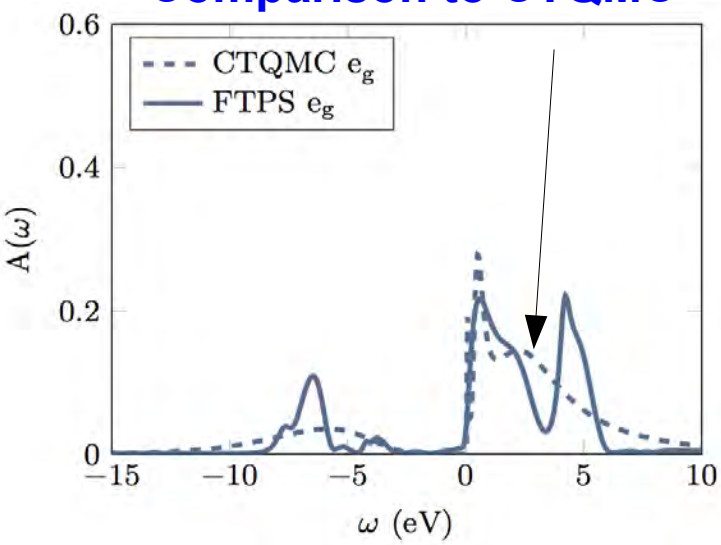

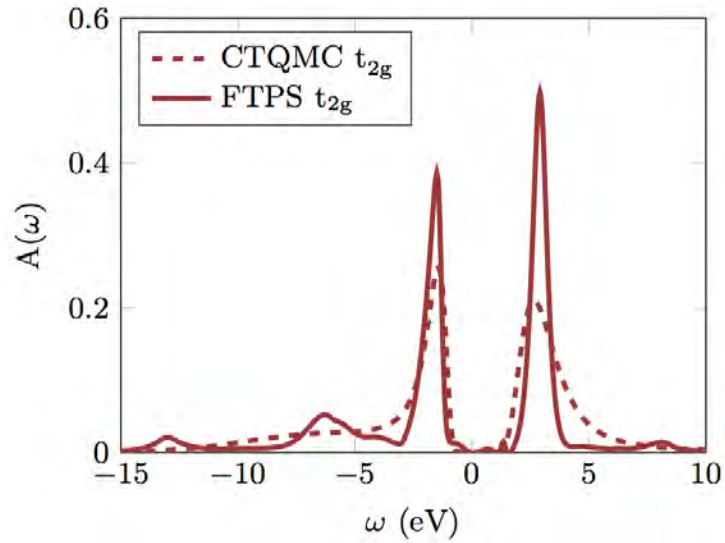

DMFT: t_{2g} plus e_g

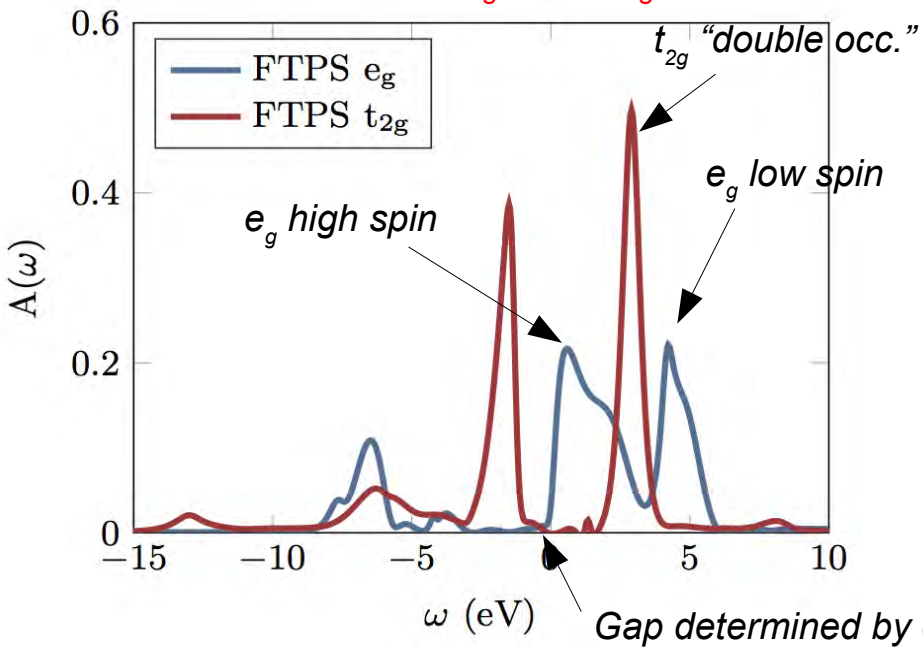

FTPS: 700 CPU-h, CTQMC: 600 CPU-h

$SrMnO_3$: t_{2g} and e_g orbitals

- Full 5-band calculation (U=6.0, J=0.8)

- e_g is important:
  - determines the gap
  - creates 3-peak structure above E_F
    (not resolved by CTQMC)

Comparison to experiment

DMFT: t_{2g} plus e_g

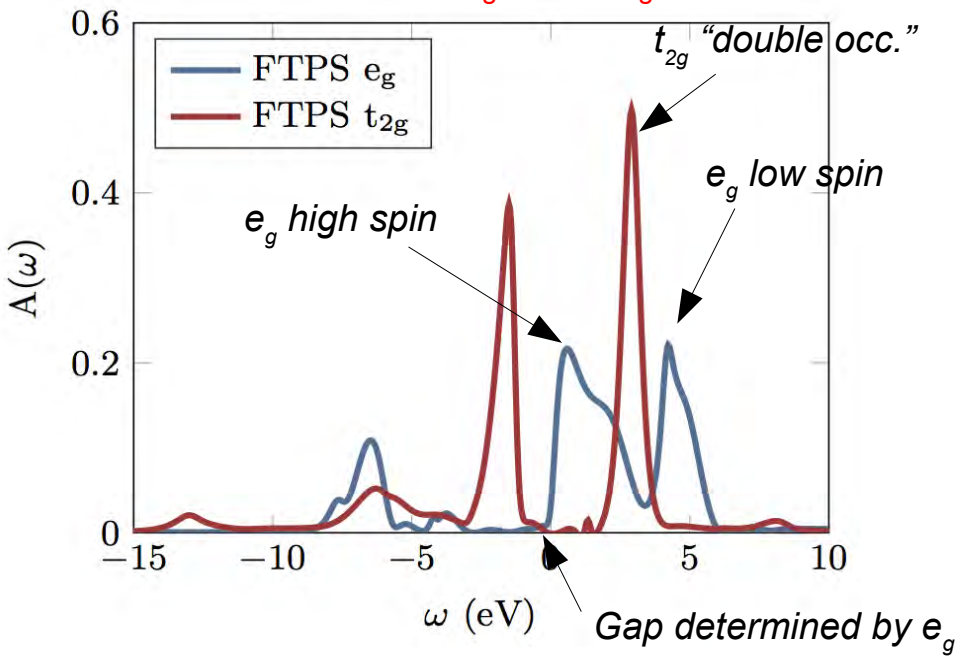

3-peak structure visible in experiment

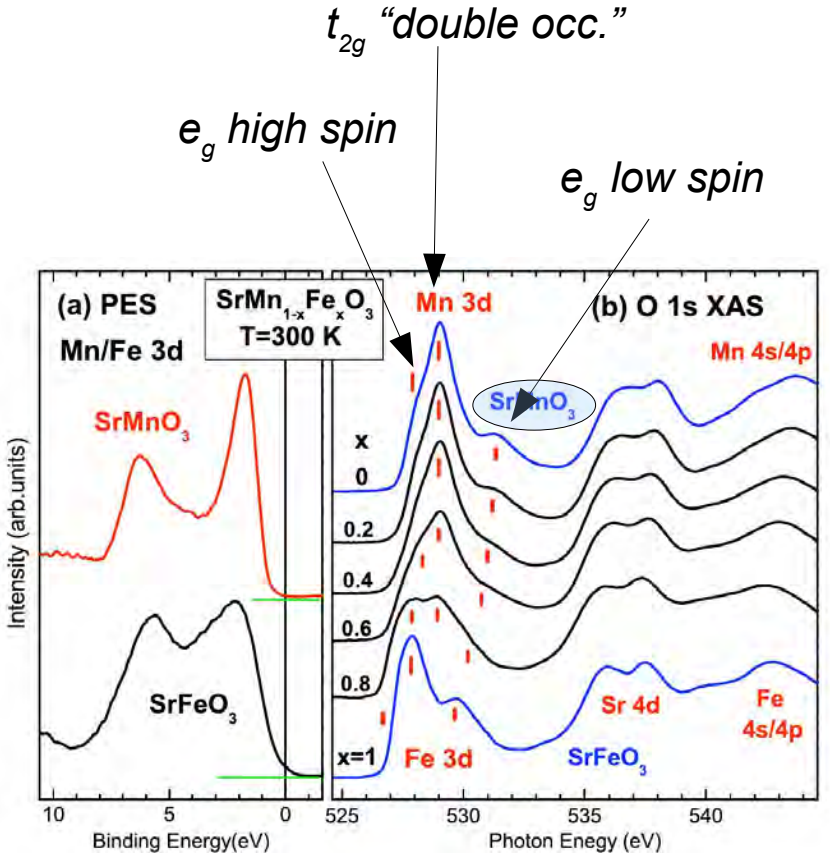

J.-S. Kang et al.,
PRB 78, 054434 (2008)

Conclusions

- **FTPS: real time impurity solver for DMFT**
  - Efficient: comparable to CTQMC
  - T=0
  - Large baths, no analytic continuation → high resolution at all energies
  - 5-orbital calculations possible
  - Can resolve multiplets in upper Hubbard band
    $SrMnO_3$: three-peak structure e_g t_{2g} e_g is also visible in experiment
- **Outlook:**
  - Non-diagonal baths, without sign problem (in preparation)
  - Nonequilibrium (in preparation) → next talk by Martin Eckstein
  - Better resolution than CT-QMC even at low energies (25meV) (→ M. Rumetshofer)
- **Limitations:**
  - Single site (so far)
  - No black box yet
  - ….